Additive Manufacturing 19 (2018) 81–94

Contents lists available at ScienceDirect

Additive Manufacturing

journal homepage: www.elsevier.com/locate/addma

Full Length Article

Strategies for functionally graded lattice structures derived using topology optimisation for Additive Manufacturing

Ajit Panesar[a,b,*], Meisam Abdi[a,c], Duncan Hickman[a], Ian Ashcroft[a]

[a] Additive Manufacturing and 3D Printing Research Group, University of Nottingham, NG7 2RD, UK
[b] Department of Aeronautics, Imperial College London, SW7 2AZ, UK
[c] Faculty of Technology, De Montfort University, LE1 9BH, UK

ARTICLE INFO

Article history:
Received 5 April 2017
Received in revised form
26 September 2017
Accepted 13 November 2017
Available online 14 November 2017

Keywords:
Lattice structures
Functional grading
Topology optimisation
Design for additive manufacturing
Finite element analysis

ABSTRACT

A number of strategies that enable lattice structures to be derived from Topology Optimisation (TO) results suitable for Additive Manufacturing (AM) are presented. The proposed strategies are evaluated for mechanical performance and assessed for AM specific design related manufacturing considerations. From a manufacturing stand-point, support structure requirement decreases with increased extent of latticing, whereas the design-to-manufacture discrepancies and the processing efforts, both in terms of memory requirements and time, increase. Results from Finite Element (FE) analysis for the two loading scenarios considered: intended loading, and variability in loading, provide insight into the solution optimality and robustness of the design strategies. Lattice strategies that capitalised on TO results were found to be considerably (~40–50%) superior in terms of specific stiffness when compared to the structures where this was not the case. The Graded strategy was found to be the most desirable from both the design and manufacturing perspective. The presented pros-and-cons for the various proposed design strategies aim to provide insight into their suitability in meeting the challenges faced by the AM design community.

1. Introduction

Cellular materials have been utilised for centuries in a wide variety of applications and are common in natural materials such as wood, bone, sponge and coral. These can be regarded as a structure that consists of a network of solid struts or plates which form the edges and faces of cells [1]. More recently these materials have been specifically designed to fulfil multi-functional material requirements in weight reduction, energy absorption, heat transfer and thermal insulation [2–5]. Conventional methods of fabricating metallic cellular materials include liquid state processing such as direct foaming and spray foaming, solid state processing including powder metallurgy sintering of powders and the use of fibres, electro-deposition and vapour deposition [6,7]. Although altering parameters of these manufacturing processes allows for some control over pore shape and size, they remain limited to producing randomly organised structures. This is in contrast to the layer-by-layer manufacturing paradigm of Additive Manufacturing (AM) which enables the creation of cellular materials with a predefined external geometry and internal architecture. Tang et al. [8] provides an overview of the various fields where cellular material designed specifically for AM are being utilised. Cellular structures designed for fabrication via AM are commonly referred to as lattice structures due to being inherently non-stochastic. Other terminology in literature includes lightweight structures and foams, while many of these terms can be used interchangeably, lattice structures has been chosen as the most accurate descriptor of the structures investigated herein.

AM enables the production of complex geometries that were previously difficult or impossible to manufacture and this has led to the creation of many different design strategies in order to manufacture parts that are both high quality, within tolerances and economic to produce [9]. Furthermore, designs can now be realised that have high specific stiffness and strength whilst reducing (or eliminating) material wastage, primarily due to AM's synergy with topology optimisation (TO), a structural optimization technique that iteratively improves the material layout within a given design space, for a given set of loads and boundary conditions [10,11]. However, it is important to consider manufacturing specific factors when designing for AM, these include: requirement for support material, limitations in build angle, wall size, hole size and dimensional accuracy [12,13].

* Corresponding author at: Department of Aeronautics, Imperial College London, SW7 2AZ, UK.
E-mail address: a.panesar@imperial.ac.uk (A. Panesar).

https://doi.org/10.1016/j.addma.2017.11.008

There have been many approaches proposed for creating optimised lattice structures. Brackett et al. [14] suggested mapping volume fractions of the lattice unit cells onto the intermediate densities of an un-penalised SIMP solution, making the greyscale density solution of TO possible to manufacture with AM. This work utilised the tessellation of the unit cell for the lattice generation, i.e. where a selected unit cell template is tessellated across the design domain in a regular fashion. Cheng et al. [15] presented a method where the density distribution from TO results were used to obtain the radii values (employed for the creation of strut members) at the vertices of the unit cells to allow the material grading of a tessellated lattice structure. Teufelhart and Reinhart [16] optimised the strut diameters of an irregular lattice structure by capitalising on the flux of force within a solid structure. They showed that enhancement in performance can be achieved when compared to a regular (uniformly tessellated) counterpart, mainly due to a much smoother distribution of stresses owing to the stress conformal nature of the lattice. To generate lattice with varying cell sizes, Brackett et al. [17] offered an error diffusion based method which enabled the mapping of irregular unit cell lattice onto a greyscale input. This was achieved by generating dithered points from the greyscale image followed by connecting them, using either Delaunay triangulation or Voronoi tessellation.

Generic ground truss structure approaches [18–20] have also been investigated for lattice optimisation, with some focused on AM [21]. Heuristic methods where unit cells are chosen from a predefined library and subsequently subjected to size optimisation to support different stress states (within a structure) have also been developed to create conformal lattices [22]. Alzahrani et al. [23] progressed the above-mentioned heuristic method further to utilise the relative density information obtained from TO to automatically determine the diameter of each individual strut in the structure. They found the method capable of producing reliable structures under multiple loading conditions and also capable of reducing the computational cost associated with the design of these structures.

Structural optimization techniques relying on weighted objective functions have also been employed for orthopaedic implant applications that take into account multiple design objectives for lattice structures including stiffness, porosity and surface area [24]. Many fields of research including biomedical, physics and materials science, have also considered optimisation of the unit cell itself. This is either done for an individual unit cell, which is subsequently tessellated throughout the design volume, or every unit cell throughout the design volume is optimised to a unique geometry. Cadman et al. [25] provides a comprehensive review of these strategies for optimised material design for a broad range of multi-functional and multi-disciplinary applications, such as, phononic/photonic bandgap materials, metamaterials, tailored fluid permeability and diffusivity, negative Poisson's ratio, conductive properties and functionally graded materials.

Recent advances in software targeted towards computer aided design and design for AM have provided new ways to design lattice structures. Some notable tools in this regard are Rhino (Rhinoceros 3D) [26], 3-Matic (Materialise) [27], Simpleware (Synopsys) [28], Within (Autodesk) [29] and Optistruct (Altair) [30]. Rhino (McNeel) provides a platform for a variety of plugins and add-ons including; a version of Symvol (Uformia) [31] that provides an F-Rep based tool that can create complex lattice structures, and Grasshopper a plugin that provides a graphical scripting platform increasing the simplicity in creating complex designs. 3-Matic, Simpleware and Within have features that are designed specifically to aid in the design of lattice structures, such as unit cell libraries and the ability to create structures with a graded density. However current versions of these software lack the ability to map lattice onto an imported (or generated) 3D density map resulting from a TO. Optistruct is the only one that offers the ability to include graded lattice structures as part of the optimisation routine, however the current implementation remains limited to only one type of cell (defined by the edges Tetrahedron).

It can be seen, therefore, that although the design freedoms offered through AM allow for the creation of complex lattice structures, the development of effective strategies to design them is an ongoing area of research. Lattice structures can be exploited in AM for many reasons including: enabling the fabrication of a TO solution with intermediate densities (as found in density based methods); reducing part distortions, as their inherent porosity minimises residual stresses, and as a result require fewer supports (support needs are alleviated with inclusion of self-supporting unit cells [32]); and improved design robustness. Therefore embracing lattice structure in design can be useful when considering both the mechanical performance and manufacturing aspects of AM design.

This paper aims to demonstrate that a closer interplay between lattice design approaches and TO is the next step in realising optimal lattice designs for AM. Therefore this work focuses on defining strategies that allow for the realisation of lattice structures that are derived using TO solutions; and benchmarking their performance in terms of both the load-bearing capability and the AM specific design related manufacturing considerations. The novelty of this work is in utilising the TO-to-lattice mapping, presented by the authors in [14], to derive differing lattice strategies and indicate their relative performance. The paper takes the following structure: firstly, differing strategies for realising lattice structures are defined, the rationale behind them and details of lattice generation, is presented; secondly, criterion for the mechanical performance evaluation and the metrics employed for assessing the AM specific design related manufacturing considerations are detailed; thirdly, results are presented and the strengths and weaknesses of the different strategies discussed; and lastly, with the aim to better equip designers and engineers, insight backed by quantitative investigation into the suitability of proposed lattice strategies for different objectives is provided.

2. Methodology

2.1. Methodology: realising lattice designs

This section comprises of three subsections: the first provides details on the TO procedure that underpins the realisation of lattice strategies, the second introduces the various proposed strategies, and lastly the details on generating a lattice structure with functionally grading is provided.

2.1.1. Obtaining optimal topologies: discrete solid-void structures and greyscale density solutions

Solid Isotropic Material Penalisation (SIMP) method [10,33] – a density-based approach where the material distribution problem is parametrised by the material density distribution to obtain optimal topologies was chosen for the TO procedure because the SIMP implementation enables results in two forms, one that allows for efficient discrete solid-void representation and the other in the greyscale density representation.

The objective of the SIMP implementation used here is to identify the optimal distribution of material density, subjected to target volume constraint, to minimise structural compliance (a measure of the inverse of stiffness). The objective function is defined as:

$$\boldsymbol{C} = \frac{1}{2}\boldsymbol{U}^{\boldsymbol{T}}\boldsymbol{K}\boldsymbol{U} \tag{1}$$

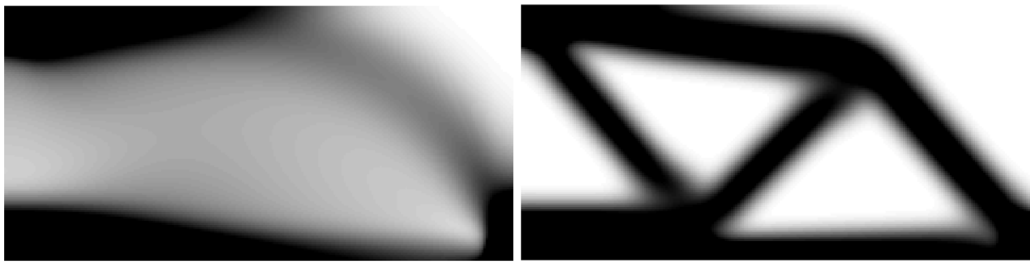

a) b)

Fig. 1. Results from SIMP for volume fraction constraint of 0.5 when penalty exponent (φ): a) set to '1′ and b) set to '3'.

subject to:

$$\boldsymbol{V}^{*} - \sum_{\boldsymbol{i}=1}^{\boldsymbol{N}} \boldsymbol{V_i \rho_i} = 0 \tag{2}$$

where C is the compliance, K is the global stiffness matrix and U is the global displacement vector, Vi is the elemental volume, N is the total number of elements, V* is the target structural volume, and elemental density 'ρi' ∈ [ρmin, 1]. For this work, ρmin was set at 1e-6. The material interpolation scheme used is as follows:

$$\boldsymbol{E}(\boldsymbol{\rho_i}) = \boldsymbol{E}_1 \boldsymbol{\rho_i^{\varphi}} \tag{3}$$

where E_1 is the Young's modulus for the solid region, and φ is the SIMP penalty exponent. In the iterative TO design process, the SIMP penalty scheme assumes an interpolation rule to penalise the intermediate densities so as to reveal part-solid part-void regions which are amenable for realising real materials or indeed lattice structures.

The sensitivity of the objective function with respect to the change of i^{th} element density is

$$\partial \boldsymbol{C} / \partial \boldsymbol{\rho_i} = -\boldsymbol{\varphi \rho_i^{\varphi - 1}} \frac{1}{2} \boldsymbol{u_i^T k_i^0 u_i} \tag{4}$$

where k_i^0 denotes the stiffness matrix and ui represents the displacement vector for the ith element. A numerical implementation of [34] utilising the optimality criterion method was employed to obtain the SIMP solutions on a mesh with equally sized cubic elements. The penalty exponent (φ) was set to 1 to obtain grey-scale density representations and a value of 3 for φ was chosen when a discrete solid-void representation was desired (see Fig. 1). The discrete solid-void representation is obtained by thresholding the density results with an iso-value of 0.5 utilising the iso-surface function in MATLAB [35].

2.1.2. Introduction to lattice design strategies

As discussed earlier, there are several approaches to realise lattice solutions. Herein, a unit cell tessellation approach is adopted, similar to that presented by the authors in [36]. Since this work focuses on studying the strategies for lattice generation, unpenalized SIMP solutions are chosen to be interpreted instead of those obtained with a unit cell specific penalisation exponent, making the material density to lattice mapping cell-type independent. A range of lattice concepts, generated using either the discrete solid-void or the greyscale representations of the TO results are illustrated in Fig. 2. The three principally differing strategies that embrace a lattice structure within a topology optimised solution are:

1) "Intersected Lattice" (Fig. 2b) – obtained from intersecting a discrete solid-void TO solution with a uniform material density lattice that fills the entire design domain. A uniform material density lattice comprises of unit cells that have a constant volume fraction '' (ratio between material volume and the volume of the design space).
2) "Graded Lattice" (Fig. 2c) – mapping a lattice with varying material density onto the greyscale density solution of TO such that density values below the V_f^{lower} bound attain = 0 (i.e. no material) and those above V_f^{higher} bound attain = 1 (i.e. fully solid).
3) "Scaled Lattice" (Fig. 2d) – mapping a lattice with varying material density onto a re-scaled greyscale density solution of TO such that the density values are bounded between [V_f^{lower}, V_f^{higher}].

Table 1
Quality descriptors indicating most to least promising candidates when considering designs of Fig. 2 for several objectives.

Design Strategy	Solution optimality	Design effort	Support requirements
Solid	*Most*	*Less*	*Most*
Intersected	*Somewhat*	*Somewhat*	*Somewhat*
Graded	*More*	*Most*	*More*
Scaled	*Less*	*More*	*Less*
Uniform	*Least*	*Least*	*Least*

At the two extremes of this spectrum are the "Solid" (Fig. 2a) and "Uniform" (Fig. 2e) strategies which show a topology optimised solid solution and an uniform material lattice that fills the entire design domain, respectively. It is of note that both Graded and Scaled strategies fall directly under the category of functionally graded lattice structures and if material grading is not the most important aspect then Intersected strategy could be included as well.

It is possible to intuitively assess the design strategies of Fig. 2 for: i) solution optimality –attainment of highest specific stiffness, ii) design effort – ease in realising the final structure, and iii) support structure requirements. Table 1 uses qualitative descriptors to rank these design strategies from least to most promising candidates when considering the above-mentioned three categories. Optimality of a solution can be estimated by evaluating its extent of deviation from the original TO solution. For example, between Graded and Scaled strategies, the former more closely interprets the TO greyscale results by permitting solid and void regions to exist whereas this is not permissible in the latter, therefore diminishing its optimality. When measuring the design effort, the number of steps involved and their associated intricacies needs to be considered. For instance, both Solid and Uniform strategies utilise a single step operation (TO and Tessellation respectively) but the former outweighs the latter in terms of the effort needed. This is due to the (somewhat demanding) underlying optimisation procedure of the former as compared to the relatively straight-forward generative design step of the latter. All the other lattice strategies build upon the solution of TO and therefore have added steps which increases their design effort. Capturing the geometric complexities that necessitate support gives a good estimate of support requirements for a design. Solid solutions from TO can often resemble

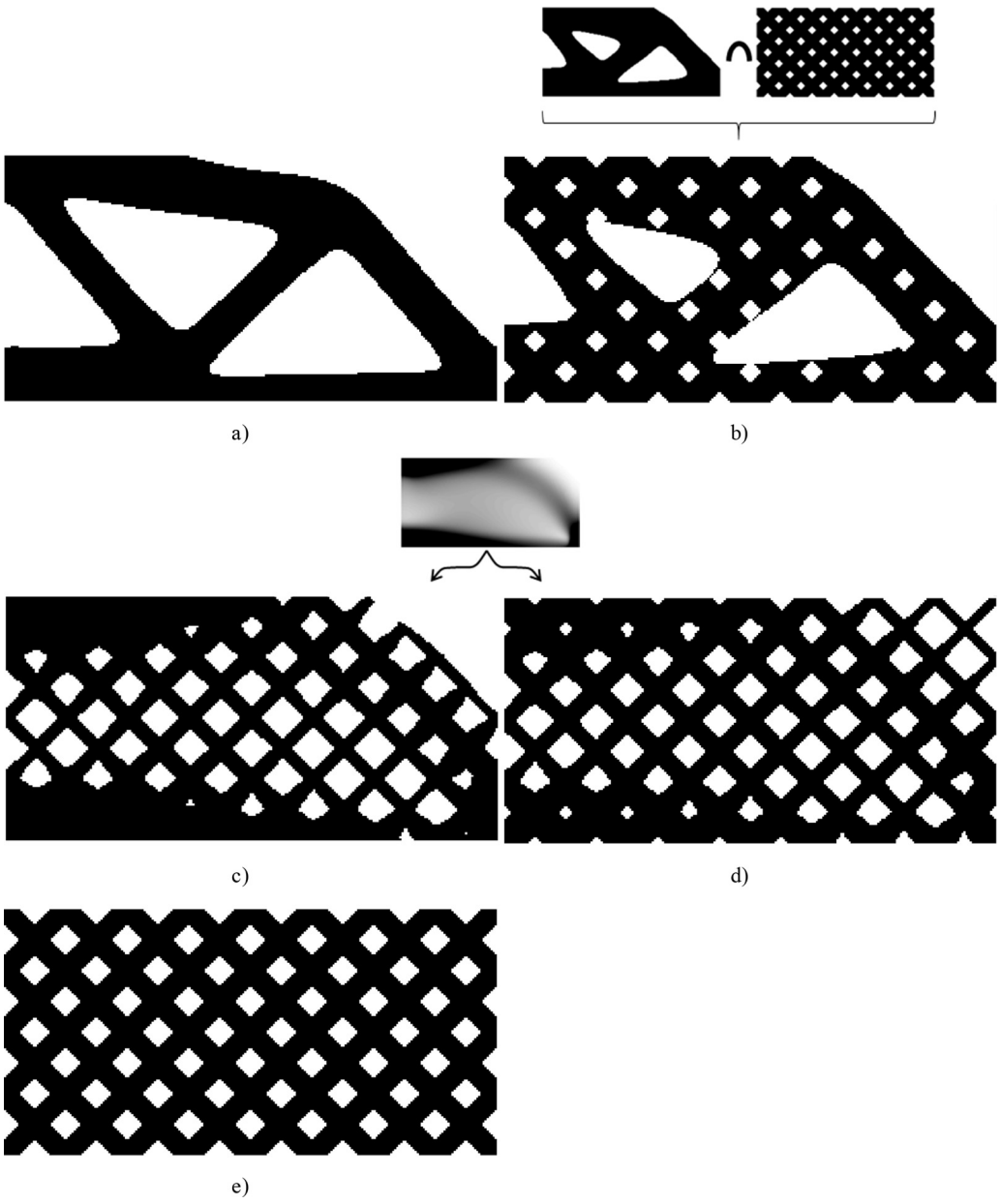

Fig. 2. Representative structures with a volume fraction of 0.5: a) Solid (SIMP solution), b) Intersected Lattice (derived by intersection Solid SIMP solution with Uniform Lattice, where both had a similar volume fraction of ~0.707 i.e. sqrt(0.5)), c) Graded Lattice, d) Scaled Lattice, and e) Uniform Lattice.

organic shapes and necessitate additional material as support for a successful build. With the inclusion of self-supporting unit cells to generate lattices derived from TO solutions, like the Intersected and Graded strategies, the need for support is alleviated. For Scaled and Uniform strategies, that fill the entire design domain, one can expect no (or base-line minimum) need for supports.

2.1.3. Generation of functionally graded lattices

Broadly speaking, lattice unit cells can be constructed using a) strut based members as shown in Fig. 3 or b) surface based representation, for example, the Triply Periodic Minimal Surfaces (TPMS) of Figs. 4–6.

The nomenclature for the library of strut based unit cells presented in Fig. 3 is as follows: BCC is Body Cantered Cubic; BCCz is BCC with 'z' direction reinforcement; FCC is Face Centred Cubic; FBCC results from the union of FCC and BCC; and names with 'S' prefix are self-supporting variants which have no members that lay parallel to the x−y plane. Strut based unit cells can be generated by specifying a strut diameter (or iso-value) for the signed distance function created over the 1D topology of the unit cell (i.e. connectivity of the vertices).

TPMS can be defined by implicit functions (i.e. $f(x, y, z) = t$) where the isovalue 't' governs the offset from the level-sets (i.e. when function value equals zero) [37]. The nomenclature for the library of TPMS presented in Fig. 4 is as follows: 'G' is Schoen's Gyroid; 'P' is Schwarz's Primitive; 'D' is Schwarz's Diamond and 'W' is Schoen's iWP. The reader is directed to [38] for further background information on the TPMS and their governing equations.

In practice, surface representations of TPMS with inequality conditions are used to generate solid structures, for instance, expressed as

$$\boldsymbol{f}(\boldsymbol{x}, \boldsymbol{y}, \boldsymbol{z}) \leq \boldsymbol{t} \tag{5}$$

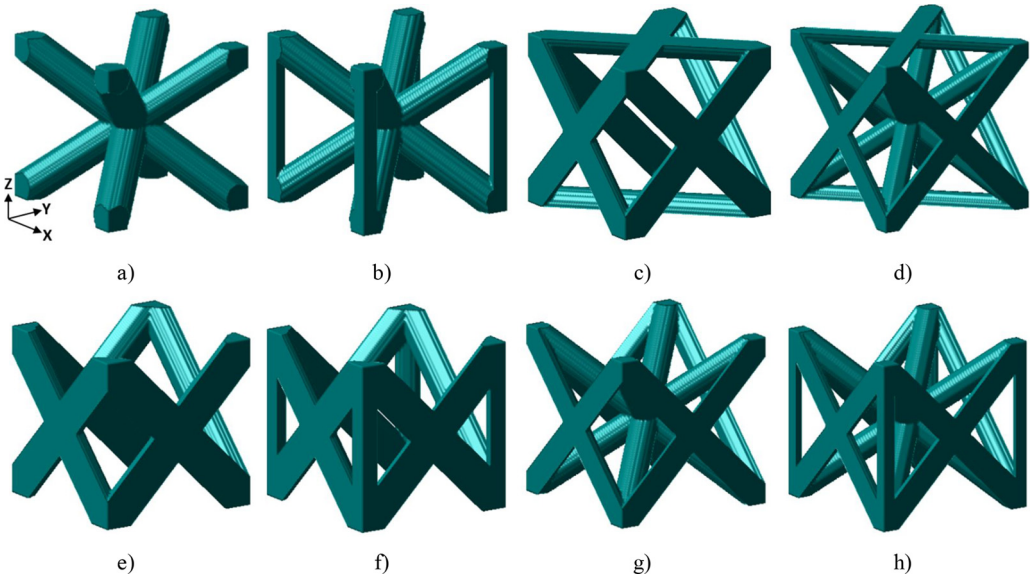

Fig. 3. Library of truss based unit cells ($V_f = 0.2$): a) BCC, b) BCCz, c) FCC, d) FBCC, e) S-FCC, f) S-FCCz, g) S-FBCC, and h) S-FBCCz.

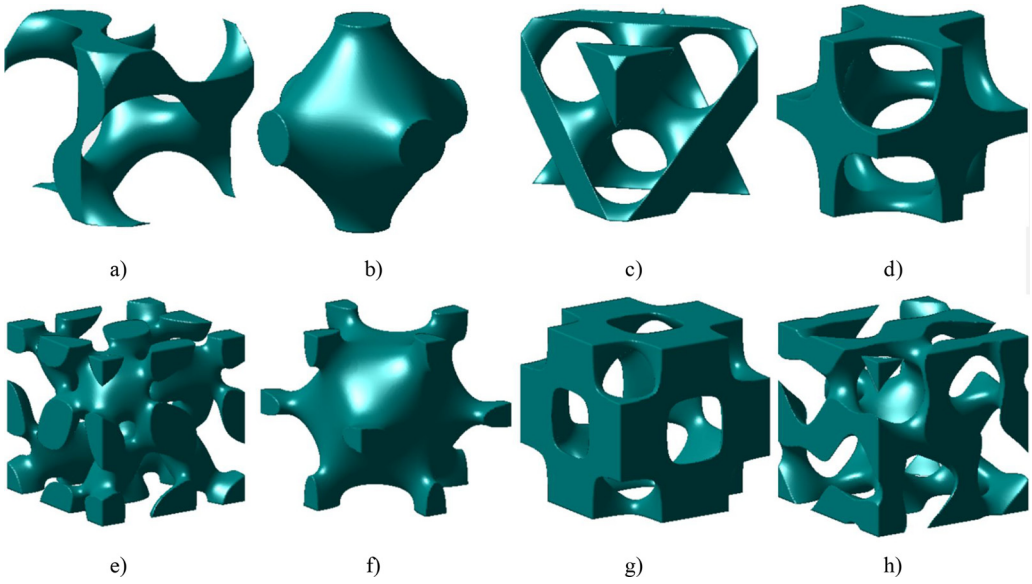

Fig. 4. Library of (implicit) surface based unit cells – Network phase (representatives): a) G (Schoen's Gyroid), b) P (Schwarz's Primitive), c) D (Schwarz's Diamond, d) W (Schoen's iWP), e) Lidinoid (by Sven Lidin), f) Neovius (by Schoen's student Neovius), g) Octo (by Schoen), and h) Split P.

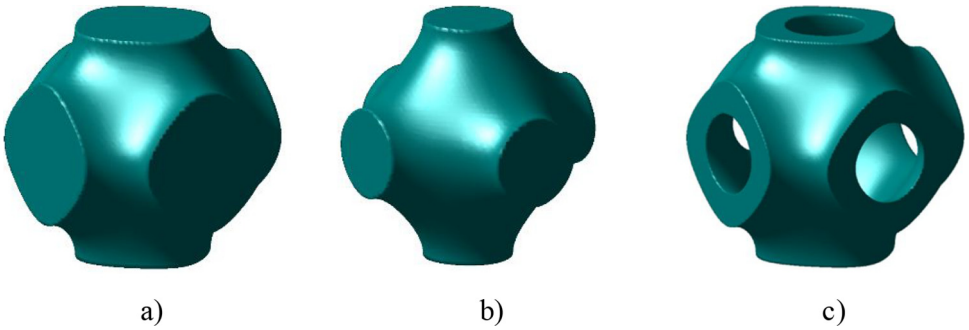

Fig. 5. Schwarz's P surfaces (for value of t = 0.37): a) $\boldsymbol{f}(\boldsymbol{x}, \boldsymbol{y}, \boldsymbol{z}) \leq \boldsymbol{t}$, b) $\boldsymbol{f}(\boldsymbol{x}, \boldsymbol{y}, \boldsymbol{z}) \leq -\boldsymbol{t}$, and c) $-\boldsymbol{t} \leq \boldsymbol{f}(\boldsymbol{x}, \boldsymbol{y}, \boldsymbol{z}) \leq \boldsymbol{t}$.

Fig. 5a and b present the solid structures derived by utilising the inequality of (5) for the Schwarz's P surface when t = 0.37 and −0.37 respectively. The governing equation of 'P' surface is

$$\boldsymbol{f}_{\boldsymbol{p}}(\boldsymbol{x}, \boldsymbol{y}, z) = \cos(\boldsymbol{\lambda}_{\boldsymbol{x}}\boldsymbol{x}) + \cos(\boldsymbol{\lambda}_{\boldsymbol{y}}\boldsymbol{y}) + \cos(\boldsymbol{\lambda}_{\boldsymbol{z}}\boldsymbol{z}) \quad (6)$$

where, λi is the function periodicity, expressed as $\lambda i = 2\pi \times ni/Li$ (with i = x, y, z); ni being the number of cell repetitions and Li the absolute dimension for the tessellated lattice domain. The family of

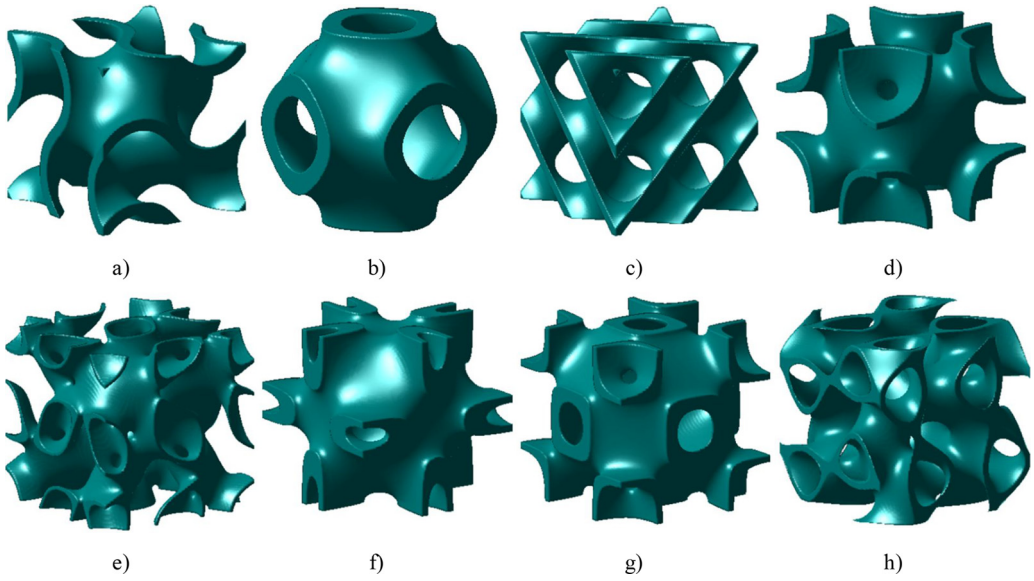

Fig. 6. Library of (implicit) surface based unit cells ($V_f = 0.2$): a) D-G, b) D-P, c) D-D, d) D-W, e) D-Lidinoid, f) D-Neovius, g) D-Octo, and h) D-Split P.

TPMS of Fig. 4 can be easily extended by defining the solid structure as

$$\boldsymbol{f}^2(\boldsymbol{x},\boldsymbol{y},\boldsymbol{z}) \leq \boldsymbol{t}^2 \tag{7}$$

i.e. $f(x, y, z)$ bounded between $[-t, t]$. These representations are commonly referred to as "Double" variant of the base TPMS and therefore have a prefix 'D' to their names (see Fig. 6). Fig. 5c presents the resulting D-P (i.e. double variant of Schwarz's Primitive) structure when using the value of t = 0.37. It is of note that the D-P structure is in effect the subtraction of Fig. 5b from Fig. 5a as this is what the inequality of (7) dictates.

Double variants of TPMS, besides having the matrix phase where $-t \leq f \leq t$ have two more solid representations resulting from $f < -t$ and $f > t$. These non-intersecting manifolds that sandwich the matrix phase are often referred to as the network phases. In this work only matrix phase structures are investigated, due to their resemblance to load bearing thin-walled structures.

Material grading of a 3D structure can be achieved by operating on a 4D representation in (x, y, z, t)-space. From an implementation standpoint, one could consider stating the material grading to be similar in form to that of Eq. (5) therefore resulting in

$$\boldsymbol{f}(\boldsymbol{x},\boldsymbol{y},\boldsymbol{z}) \leq \boldsymbol{t}(\boldsymbol{x},\boldsymbol{y},\boldsymbol{z}) \tag{8}$$

Here, t is an isovalue matrix in the (x, y, z)-space that controls the volume fraction (or V_f) variation for the lattice structure within Cartesian space. The relationship between t and V_f were obtained for various unit cells by employing curve-fitting techniques to ensure that the average volume fraction for a unit cell equated to the average volume fraction for the corresponding volumetric region within material density/grading map. Each voxel (volumetric pixel) for evaluation assumed homogenised properties with field values at the element centroid. Fig. 7 shows an example of linear grading for BCC and D-P unit cells where V_f varies from 0.1 at the bottom to 0.5 at the top of the lattice structure.

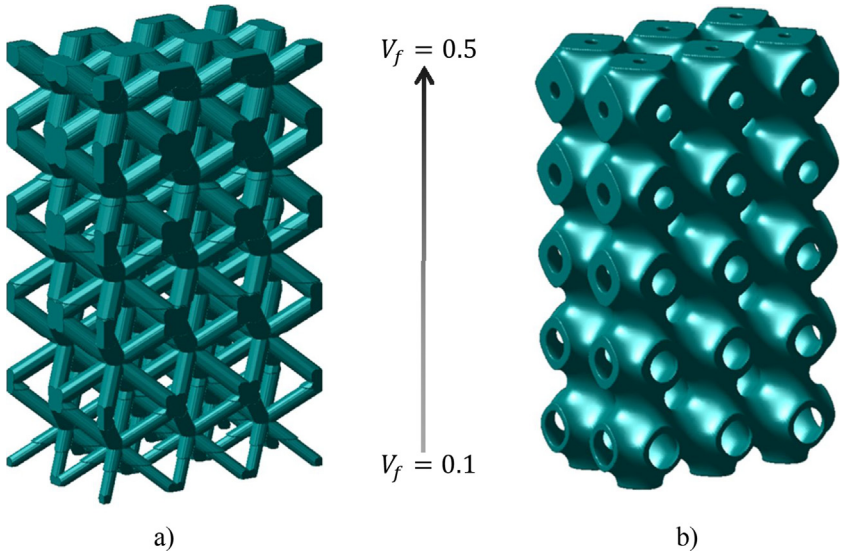

Fig. 7. Example of a linear material grading for: a) strut based BCC lattice and b) surface based D-P lattice.

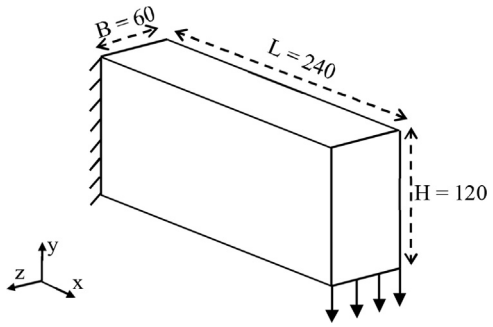

Fig. 8. 3D Cantilever problem.

2.2. Methodology for numerically evaluating the mechanical performance of design strategies

Most studies concerning TO methods consider the classic cantilever plate (in 2D) or beam (in 3D) problem and therefore this work also utilises such a structure (see Fig. 8 with a design domain of $240 \times 120 \times 60$ voxels/units) to investigate the proposed design strategies. For obtaining lattice structures unit cells occupying a $20 \times 20 \times 20$ voxel cube were used, resulting in structures comprising of $12 \times 6 \times 3$ unit cells. Mechanical performances were evaluated for two loading scenarios: defined loading (i.e. intended loading), and defined loading with uncertainties (i.e. variability in loading). Total Strain Energy (SE) of the structures was used as the performance measure – a lower SE indicate a more efficient (stiff) structure.

The structures of Fig. 9 were used for the numerical investigation and had a total V_f of 0.5. The lattice variants utilised bounds V_f^{lower} of 0.3 and V_f^{higher} of 0.85. Doing so, ensured that the finite element models had a minimum of 3 element thick wall/struts in the lowest V_f regions and this was noticed to adequately capture the unit cell behaviour in the mesh refinement study (convergence of displacement values under the cantilever loading case). For Fig. 9b and c, SIMP solid-void solutions obtained with a total V_f of 0.7 were used to intersect with a constant V_f lattice of 0.715 resulting in average structural V_f of 0.5.

Loading scenario – I: Defined loading corresponds to the case when a unit load vector is along −y axis (i.e. $F = [0, -1, 0]$) as shown in Fig. 8.

Loading scenario – II: Defined loading with uncertainty aims to assess the robustness of the design strategies by considering uncertainties or variabilities in the defined loading. Two forms of variability, one that captured the directionality of this load vector and the other that investigated the influence of the% contribution of this load vector along the y axis were studied. The former is represented by F_i (where, i = 1, 2, 3) and the latter by F_j (where, j = L, H). The% x,y,z component values for the considered unit load vectors are reported in Table 2. Structures were loaded under all of the specified 15 cases and in each case had the dominant vector component along the '–y axis'. Where this contribution is higher than 95% of the load vector magnitude (unity), the load variability is referred as lower and is denoted by F_L. Conversely, for higher variability associated with contributions under 95% along '–y axis', the term F_H is used. To assess the effects of directionality, F_1 utilises second dominant loading along the '–z axis', F_3 along the −x axis and F_2 considers equal components about the '–x and −z axes'.

All structures were analysed using hexahedral elements filling the entire design domain with an edge length of one voxel/unit resulting in a mesh comprising of 1.728 million elements. Finite Elements (FE) representing solid regions were assigned a moduli of unity and those representing void regions assigned the much lower value of 1e-6 (soft-kill approach). The value for the Poisson's ratio was chosen as 0.3. A commercial FE solver, specifically MSC Nastran [39], was used to calculate the total SE to inform the mechanical performance.

2.3. Methodology for assessing the design related manufacturing considerations for the various design strategies

In addition to the mechanical performance evaluation of the presented design strategies, this study investigates a number of design related manufacturing considerations, specifically, manufacturing issues that can be tackled to some extent by modifying a design. The data for comparison was collected from processing the solutions using 3D printing software such as Magics [40] and Autofab [41]. The three criteria investigated in this study consist of: i) support structure requirement, ii) processing effort, and iii) design-to-manufacture discrepancy.

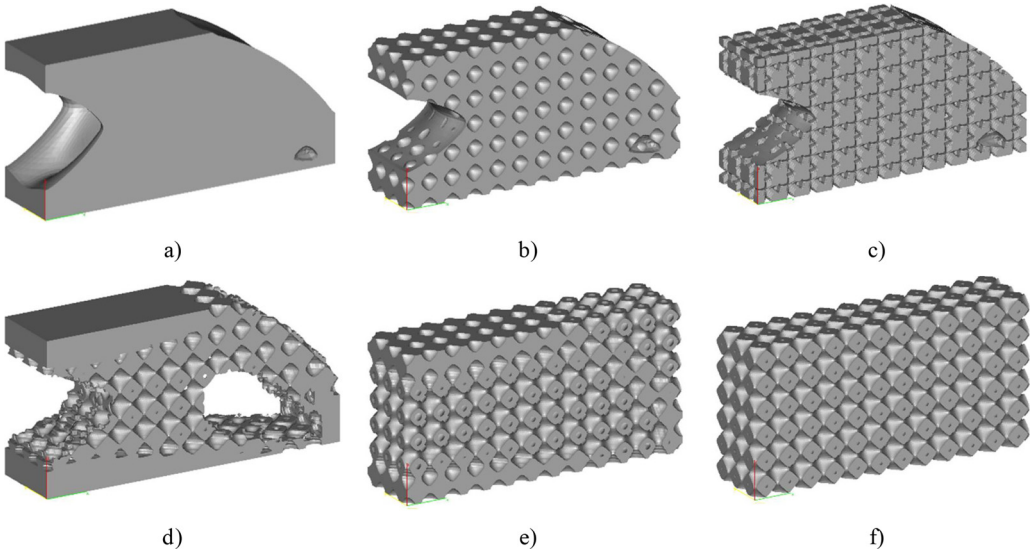

Fig. 9. Structures used for FEA: a) Solid (SIMP solution), b) Intersected Lattice of D-P, c) Intersected Lattice of BCC, d) Graded Lattice of D-P, e) Scaled Lattice of D-P, and f) Uniform Lattice of D-P.

Table 2
% x,y,z components of the considered unit load vectors for the loading scenario II.

	$-F_1$			$-F_2$			$-F_3$		
	x	*y*	*z*	*x*	*y*	*z*	*x*	*y*	*z*
Lower variability (F_L)	0	99	1	1	98	1	1	99	0
	0	96.9	3.1	1.9	96.2	1.9	3.1	96.9	0
	0.9	94.1	5	3	93.9	3	5	94.1	0.9
Higher variability (F_H)	2.1	92.2	5.8	4.2	91.6	4.2	5.8	92.2	2.1
	0.5	88.3	11.3	5.6	88.9	5.6	11.3	88.3	0.5

An important consideration when designing parts for metal AM, specifically Selective Laser Melting (SLM), is the support structure requirement. In general, downward sloping faces with an angle of 45° or less require support structures [42], and additional support reinforcement may be needed in regions that experience high residual stress due to the build process in order to prevent part distortion. Although over-supporting a component can reduce the chance of a build failure, it increases the manufacturing time, the powder used, and the post-processing efforts for support removal. The aim of the support structure investigation in this study is to compare the relative support structure needs for the different design strategies. Similar to [43], a fixed build orientation, i.e. y axis (or the loading direction) is chosen as it provided greater scope for comparing the support structure requirement when compared to x and z axes whilst keeping similar build times. It is of note that by identifying the optimal build direction for each design, minimal support needs specific for a design can be obtained precisely. Such an investigation is beyond the scope of this work and therefore a fixed build orientation is employed for the relative comparison.

To quantify the support requirement for the different designs, Magics support generation module was employed. The surface area of the overall support in a structure was used as a measure for support requirements. The different designs were added to a scene representing a Realizer SLM50 build platform and oriented with the 'y axis' normal to the build platform (refer to Fig. 15). The software automatically generated support structures using proprietary algorithms and this allowed for a fair comparison to be made of the support structure requirement for the various design strategies.

The processing efforts required for generating the suitable file format for a 3D printer (i.e. AM machine) from the design file format can be related to the geometrical complexity of the designed samples as well as the size of the file representing the samples. STeroLithography (STL) is the de-facto file format for manufacture in the AM sector. The STL file describes a part's geometry (specifically surface) using triangles, therefore, the size of an STL file is directly dependent on the number of triangles used to represent the surface and in-turn a good measure of part complexity. A large STL file specifies a greater number of triangles and as a result requires more computer memory to perform computational operations (such as Boolean operations), and also results in increased processing efforts needed to generate a sliced file format for 3D printing. To better understand the processing efforts, two measures were considered: Measure-1 – the number of triangles needed to define the geometry, and Measure-2 – the time spent on generating the sliced files of the components (in Magics). Doing so allows for investigation as to whether there is a direct correlation or dependency between the two measures.

In addition to the support requirements and processing efforts, design complexity plays a role in the design-to-manufacture discrepancy, i.e. disparity between the intended design and the manufactured part. For AM components, this disparity can be attributed to two main sources: the deflection of component due to a high residual stress, and surface roughness effects. Lattice structures when compared to solid samples for the same total volume are less affected by residual stress due to their inherent porosity but can be detrimentally influenced by the surface roughness and balling effects [44] due to the difficulties associated with performing surface finish operations. A preliminarily investigation showed that the weights of the manufactured lattice parts were found to be noticeably different from the intended designed weights (due to loosely attached powder). A second order polynomial function adequately captured the relationship between the error percentage (the above discussed disparity) and the surface area to volume ratio for a number of SLM manufactured Titanium lattice cubes samples (densities ranging from 0.1 to 0.6).

$$\varepsilon = \left|\frac{w_b - w_d}{w_d}\right| \times 100\% = -0.12\left(\frac{A}{V}\right)^2 + 7.3\left(\frac{A}{V}\right) - 4.7 \quad (9)$$

where, ε is the error%, A is the surface area, V the volume of the part, and wb and wd represent the build and designed weight of the component, respectively. In this work, Eq. (9) is used to report the disparity/error between design and manufacture for the explored design strategies.

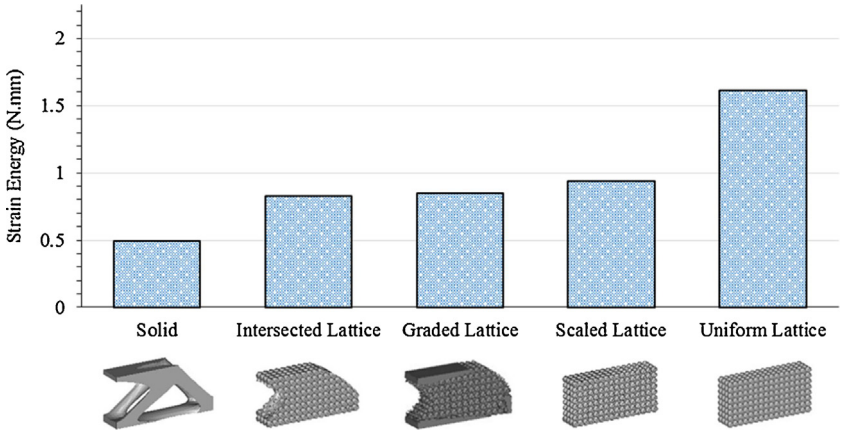

Fig. 10. Total strain energy of the various design strategies for the case of intended loading.

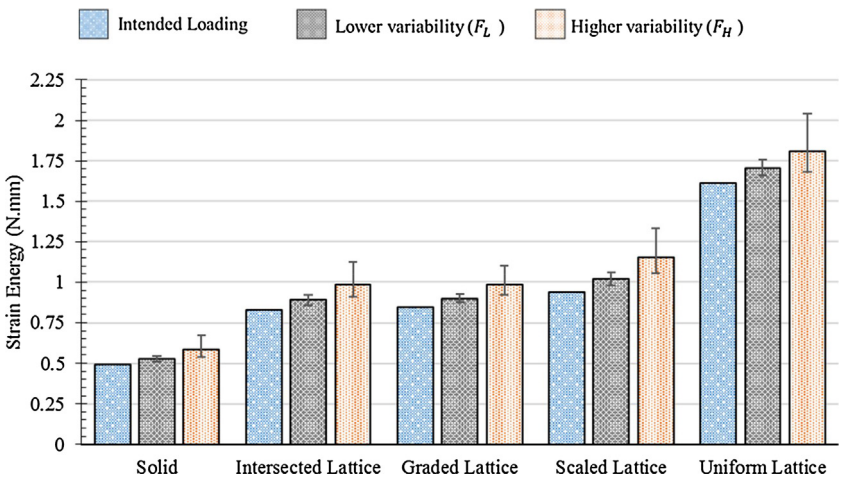

Fig. 11. Total strain energy of the various design strategies for the case of $\boldsymbol{F}_1$ variability in loading.

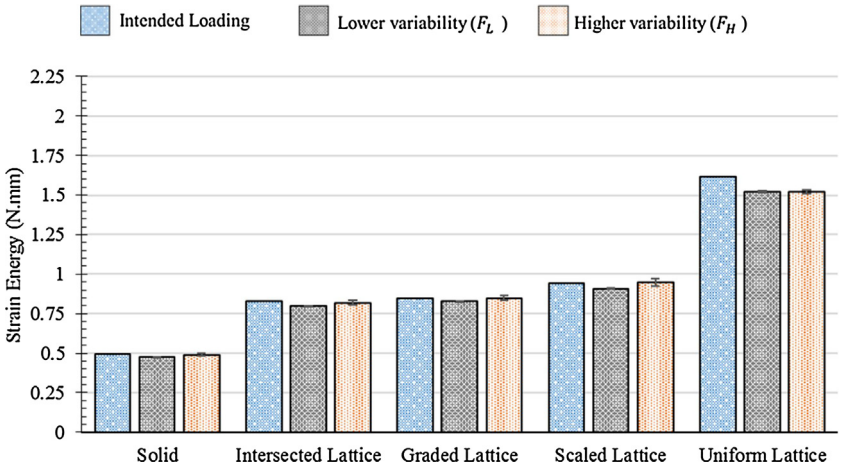

Fig. 12. Total strain energy of the various design strategies for the case of $\boldsymbol{F}_2$ variability in loading.

3. Results and discussion

3.1. Numerical evaluation

The resulting total SE for the different design strategies applied to the cantilever beam test case under intended loading are presented in Fig. 10. These results are in agreement with the intuitively predicted ranking of Table 1. The Solid solution derived from the penalised SIMP optimisation attained the lowest SE. Conversely, the Uniform lattice structure possessed the highest SE. Intersected and Graded structures gave the lowest SE values for structures embracing lattices. The Scaled lattice design gave much lower (58%) SE value than the Uniform lattice indicating a more optimal solution although the solution was noticeably inferior (~10%) to the Intersected and Graded structures. This confirms the hypothesis that a solutions' extent of deviation from the original TO solution directly relates to optimality for a chosen strategy. It is of note that the performance of an Intersected lattice, in principle, can range anywhere between a Solid and Uniform solution as the structure itself is derived by intersecting a Solid solution with a Uniform lattice but for all practical purposes it is safe to assume that this approach will employ a great deal of TO to attain superior performance.

The total SE values for the different design strategies when subjected to the loading of F_1,F_2andF_3 are presented in Figs. 11–13, respectively. For each design strategy, three columns are shown: left-most (blue colour) is the result from the intended loading case (for reference purposes), middle (grey column) corresponds to the lower variability case (F_L) and right-most (orange colour) the higher variability case (F_H). Error bars indicate the highest and lowest values, to highlight the range in response to each load and do not to indicate uncertainty.

To provide an insight into the above results, consider the simplified case of a homogenous cantilever beam of Fig. 8 which has a constant cross-section and unvarying moduli value. For such a structure, the SE values under the deformation modes outlined in Table 3 can be computed using simple analytical expressions. It is evident that the SE stored in the structure due to the bending induced by F_z is much higher than the case of stretching induced via F_x. As all loads in Table 2 have the dominant vector component along the '–y axis', therefore, the chief contributor of SE is the bending induced by the F_y load component. F_1utilised second dominant loading along the '−z axis' and therefore it has a higher SE stored in the structure indicating inferior performance (see Fig. 11) when compared to the case in which the second dominant loading is along the '−x axis' (i.e. F_3). With F_2 having equal components about the '−x and −z axes', it can be expected that the SE values lie in between the previously reported cases and this is what was observed (see Fig. 12). Although, inferences have been made using a homogenised beam, similar SE trends can be expected with the case of non-homogenous structures, like the considered lattice structures. It is worth pointing out that with changes in the relative dimensions, i.e. L:B:H ratios, assumption made about the dominant

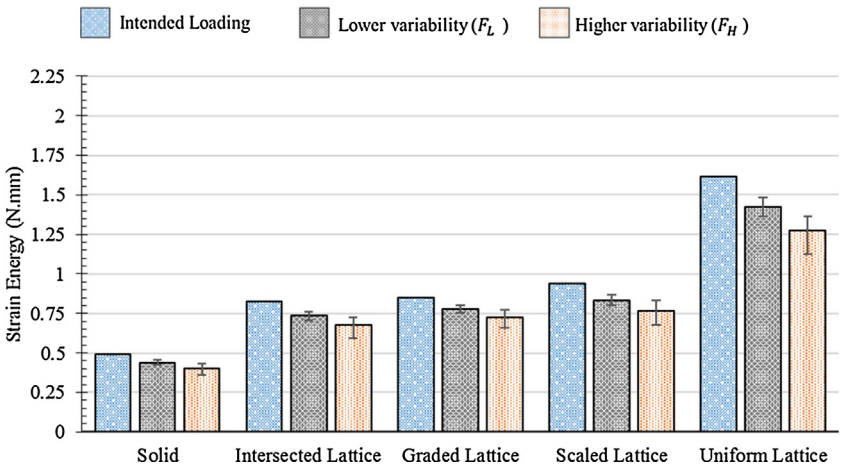

Fig. 13. Total strain energy of the various design strategies for the case of $\boldsymbol{F}_3$ variability in loading.

Table 3
Strain energy in the beam under different modes of deformation – a simplified analytical approach.

Load case	General statement for the stored SE		SE in beam of Fig. 8 (L = 4 B and H = 2B)
Stretching due to $\boldsymbol{F_x}$	$U = \int_0^L \frac{F_x.F_x.dl}{2EA}$	$= \left(\frac{F_x.F_x}{E}\right) \cdot \left(\frac{L}{2BH}\right)$	$= \left(\frac{F_x.F_x}{E}\right) \cdot \left(\frac{1}{B}\right)$
Bending due to $\boldsymbol{F_y}$	$U = \int_0^L \frac{M.M.dl}{2EI}$	$= \left(\frac{F_y.F_y}{E}\right) \cdot \left(\frac{2L^3}{BH^3}\right)$	$= \left(\frac{F_y.F_y}{E}\right) \cdot \left(\frac{16}{B}\right)$
Bending due to $\boldsymbol{F_z}$		$= \left(\frac{F_z.F_z}{E}\right) \cdot \left(\frac{2L^3}{B^3H}\right)$	$= \left(\frac{F_z.F_z}{E}\right) \cdot \left(\frac{64}{B}\right)$

Table 4
Performance resilience for design strategies.

	F_L			F_H		
	F_1	F_2	F_3	F_1	F_2	F_3
Solid	0.07	0.04	0.1	0.19	0.01	0.18
Intersected	0.08	0.04	0.11	0.19	0.01	0.18
Graded	0.06	0.02	0.08	0.16	0	0.14
Scaled	0.09	0.03	0.11	0.22	0.01	0.18
Uniform	0.06	0.06	0.12	0.12	0.06	0.21

loading scenario of Table 3 and the area moment of inertias may change making the current interpretations void.

When comparing various design strategies for F_L and F_H variabilities, the ratio of the mean SE value associated with the variable loading case (i.e. middle and right-most columns) and the SE for intended loading (i.e. left most column) can help estimate Performance Resilience (PR). Herein, PR is defined as the absolute difference between the ratio computed above and unity. The smaller the value the greater the resilience, as the performance of the structure varied the least when subject to variation in loading. Table 4 reports the PR values for the five design strategies investigated. The Graded strategy was observed to be most resilient as it attained the lowest PR values (except for F_H^1 where it was second lowest). Conversely, the Uniform strategy was found to be least resilient (except for F_H^1 where it attained a low PR value). The other three strategies attained intermediate PR values, with the Scaled strategy being marginally less resilient than the others.

In addition to the reported total SE values, review of the distribution of SE values through the use of contour maps reveals more information about how the different designs respond to loading. Scaled and Uniform lattices were compared as they both filled the entire design domain (a common feature) and only differed in the way the material was distributed within the volume. Fig. 14 shows the differences in the SE distribution between the two strategies for the case of intended loading. The Uniform lattice appears to have a greater variation in the distribution of SE and this is confirmed by the Standard Deviation (SD) values. The SD calculation utilised values that were thresholded to below the cut-off value of 1.8e-5 (the same threshold is used for the illustrations of Fig. 14). The Uniform lattice was found to have a standard deviation of 2.47 whereas the Scaled lattice was found to be only 1.36. A tighter band of SE values (i.e. lower SD) should, in principle, indicate a more optimal strategy as the load bearing capability of a structure is better utilised with most regions attaining SE values closer to the average.

When considering design approaches, different unit cell geometries form an important part of the decision making process. To highlight this, the Intersected lattice was tested with both D-P unit cells (Fig. 15a and b) and BCC unit cells (Fig. 15c and d). Visual comparison shows that the BCC cells have raised SE at the interface of unit cells. This can be considered as a feature of using a strut based lattice structure such as BCC as opposed to the surface based D-P structure. As can be seen, the D-P structure has a smoother distribution of SE. This has potential advantages in preventing failure due to stress concentrations. Stress concentrations are also visible where unit cells have been cut in void regions, this is less noticeable in the surface based design due to the higher degree of connectivity that a cut 'wall' or surface has in comparison to a cut strut member. The trends seen in the visual interpretation of SE values are supported by the numerical distribution of SE values. The BCC structure has a SD of 1.40 while the D-P structure has a SD of 1.06, when using the cut-off value of 1.2e-5 (i.e. the same threshold used for the illustrations of Fig. 15). It is of note that with the Intersected strategy, lattices can be generated by intersecting a higher V_f Solid solution with a lower V_f Uniform lattice to result in a structure comprised of thin members, leading to higher stress concentrations.

3.2. Manufacturing evaluation

Table 5 reports the "as measured" as well as "relative measure" (i.e. normalised to unity) values for the three design related manufacturing considerations explored, specifically, support structure requirement, processing efforts and design-to-manufacture discrepancy. Note: for all the data collected, structures underwent

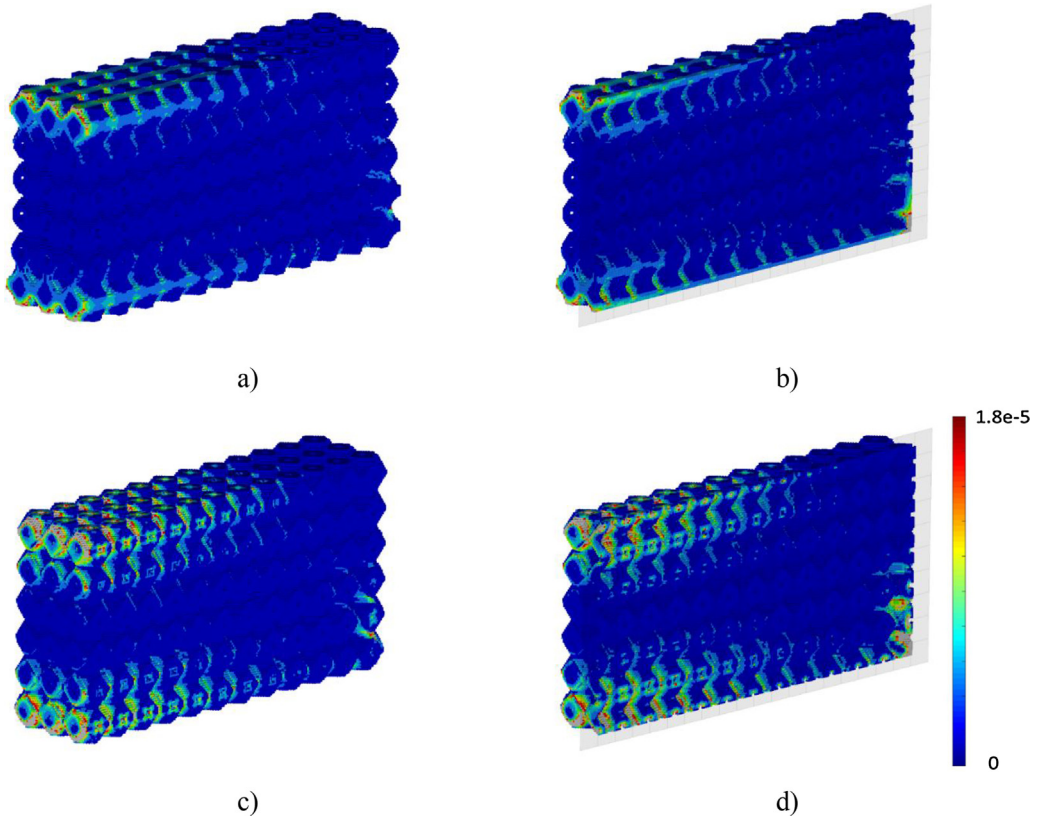

Fig. 14. Contour maps showing strain energy variation for: a) Scaled Lattice (isometric view), b) Scaled Lattice (section view), c) Uniform Lattice (isometric view), and d) Uniform Lattice (section view).

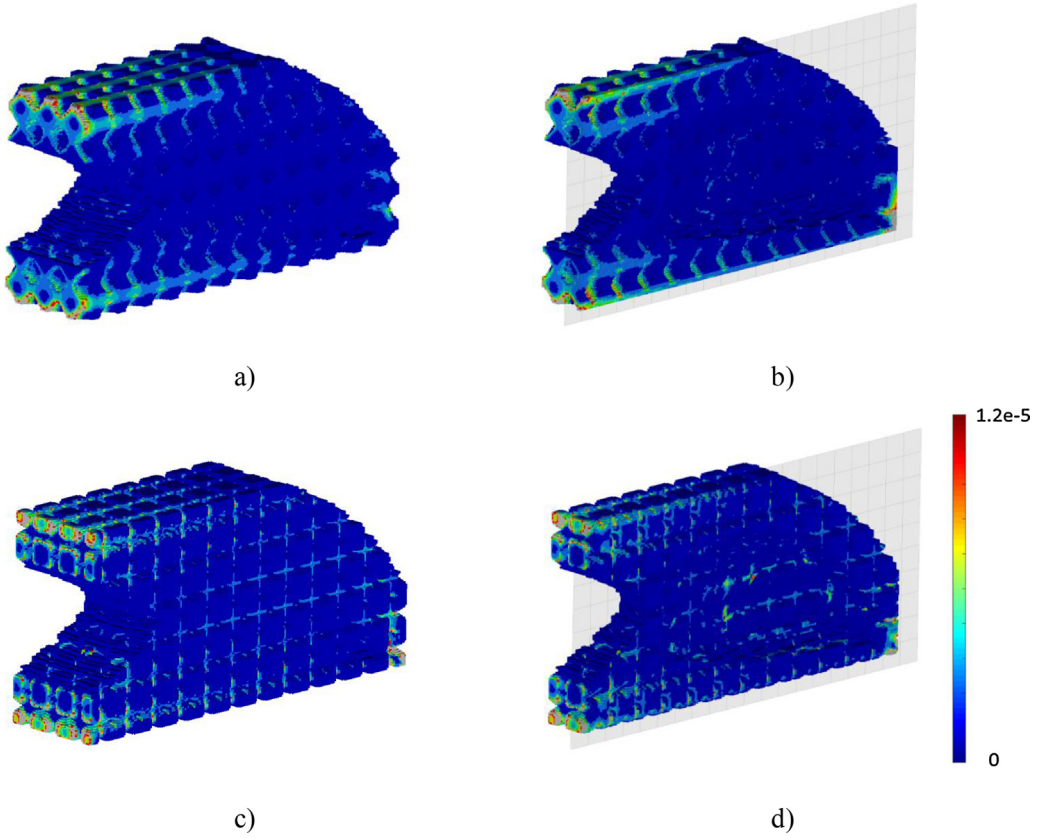

Fig. 15. Contour maps showing strain energy variation for: a) Intersected Lattice employing D-P unit cell (isometric view), b) Intersected Lattice employing D-P unit cell (section view), c) Intersected Lattice employing BCC unit cell (isometric view), and d) Intersected Lattice employing BCC unit cell (section view).

Table 5
Design related manufacturing considerations for the design strategies.

		Solid	Intersected	Graded	Scaled	Uniform
Support Structure requirement	Real value	3501	2826	2485	1509	1350
	Relative measure	1	0.807	0.710	0.431	0.386
Processing efforts	Triangles	1716	71986	110476	175794	188058
	Relative measure	0.009	0.383	0.588	0.935	1
	Time	1.8	4.3	4.4	7.3	7.8
	Relative measure	0.231	0.551	0.5641	0.9359	1
Design-to-Manufacture discrepancy	Estimated error%	0.4	3.5	2.8	8.2	8.5
	Relative measure	0.005	0.412	0.329	0.965	1

the same triangle reduction procedure (in Magics) after employing identical values for the minimum detail size.

As discussed earlier, Solid solutions from TO can often resemble organic shapes and have considerable overhang surfaces (as in Fig. 16a and b) necessitating extensive support to enable a successful SLM build. Conversely, lattice designs with self-supporting unit cells filling the entire design domain, i.e. Scaled and Uniform strategies of Fig. 16e and f, require base-line minimum supports which amounted to ~40% of the Solid case. Intermediate support requirements (70–80% of the Solid case) were observed for the Intersected and Graded strategies, Fig. 16c and d respectively, mainly due to the presence of some internal/external overhang surfaces as these strategies only fill part of the design domain with lattice.

Fig. 17 presents the relative measures reported in Table 5 in an easy to compare (pictorial) format with surface area included for reference. When moving left-to-right (i.e. Solid to Uniform strategy), a general increasing trend is observed for all the design related manufacturing considerations (except for the support require-

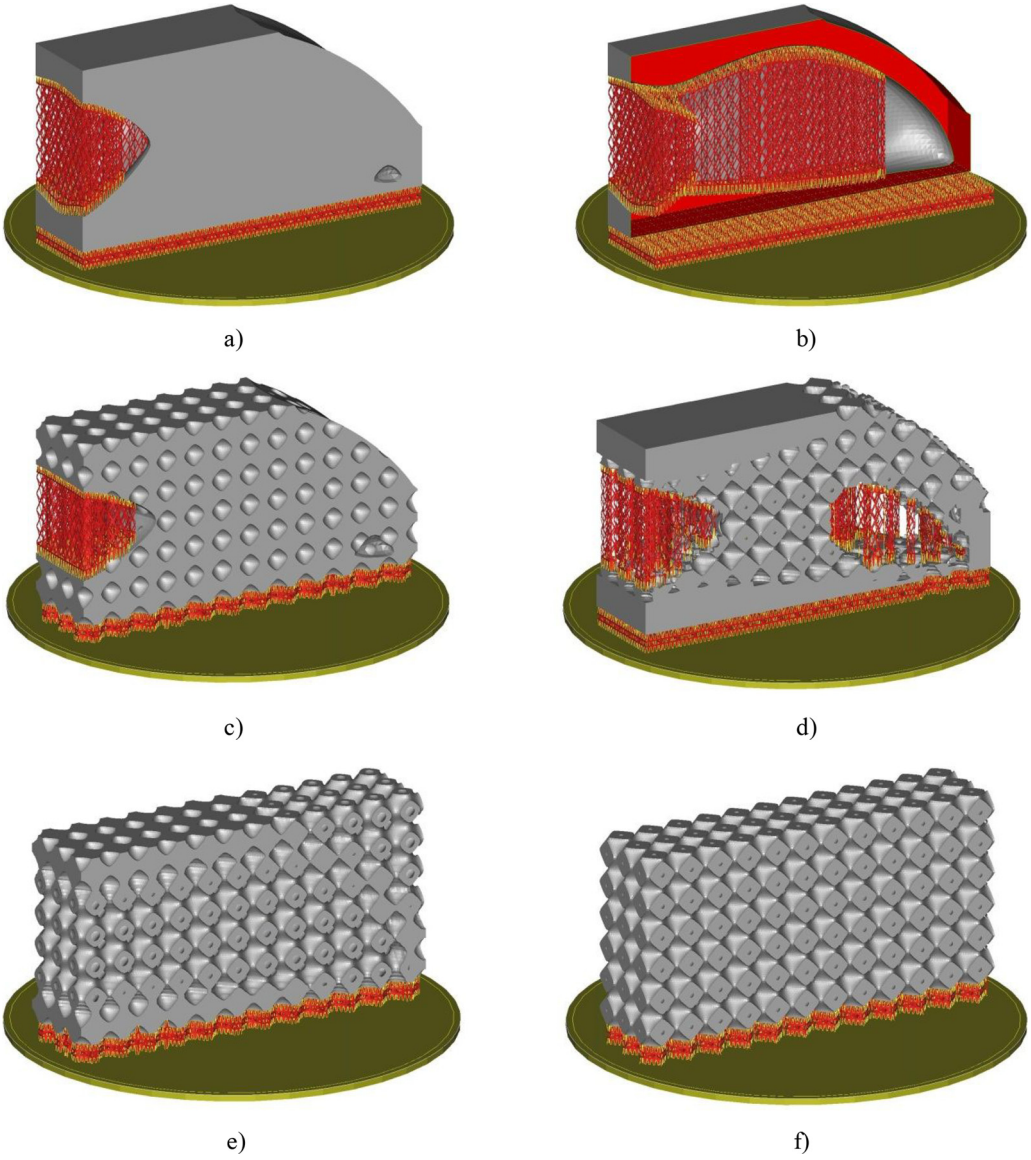

Fig. 16. Support structure requirements for: a) Solid, b) Solid (section view), (c) Intersected Lattice, (d) Graded Lattice, (e) Scaled Lattice, and (f) Uniform Lattice.

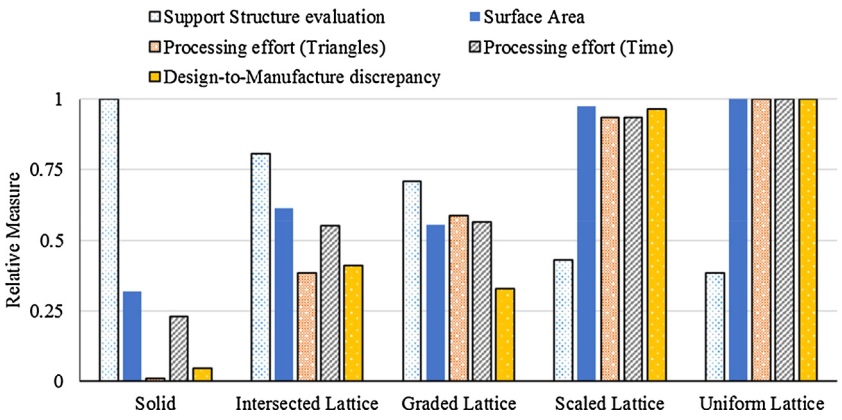

Fig. 17. Relative measure reported for the comparison of design related manufacturing considerations.

ments). In general, for the case of lattices comprised of unit cells that are not self-supporting, a similar increasing trend for support requirement can be expected since the geometric complexity that necessitates support increases with latticing. With the inclusion of self-supporting unit cells, this trend can be reversed, as shown in this investigation (and the predictive ranking of Table 1), giving confidence in the hypothesis "capturing the geometric complexities that necessitate support gives a good estimate of support requirements for a design".

It is evident that the greater the extent of latticing, the higher the surface area of the solution. Intersected and Graded lattices have nearly two-fold the surface area whereas the Scaled and Uniform lattices have almost three-fold when compared to the Solid solution. It is of note that the number of triangles needed to represent a Solid solution in comparison to Uniform lattice is greatly reduced (1/100th), due to the much simpler surface patches needed to define its geometry. Comparing Graded with Intersected lattice, although the former had marginally lower surface area (a result of accommodating solid regions), the representation of lower V_f unit cells meant a higher number of triangles were needed overall. To put things in perspective the lower V_f in Graded was 0.3 whereas the Intersected lattice utilised a uniform V_f of 0.715.

There seems to be a direct correlation between the "number of triangles" (Measure-1 of processing effort) and processing time (Measure-2) when the number of triangles exceed the 110k mark (i.e. structure achieves sufficient geometric complexity). However with triangle numbers, as is the case with Solid solution and Intersected lattice, a baseline/offset processing effort (time) needed for slicing can be seen (see Fig. 17).

Owing to the relatively low surface area of the Graded lattice when compared to other lattice designs, a low value for the design-to-manufacture discrepancy is found. It can be inferred that the Graded, amongst other lattice strategies, can produce manufactured parts that deviate the least from the intended design. It should be noted that design-to-manufacture discrepancy adds to the weight of the part, and potentially effects mechanical properties, therefore when utilising lattice structures for optimised design strategies, particularly for low density, one needs to take into account the change in the part weight after manufacturing in order to compensate for the extra weight added to the component after the build.

In addition to the AM specific design related manufacturing considerations explored above, there are several others that need to be considered when designing lattice structures for SLM. These include the minimum wall thickness that the machine can produce, and the minimum pore size for removing loose powder after the build. Therefore, for each cell type and cell size, there is a minimum and maximum density that is possible to manufacture. Another issue, is the self-supporting property of the cells which can be affected by increasing the cell size if the cell has any overhang surfaces greater than the specified limit. Evidently, this is not an issue for a BCC cell with 45° members, however, for a truss-like cell with horizontal members, e.g. FCC and FBCC, one should take this into account.

4. Concluding remarks

Topology optimisation (TO) techniques and generative lattice design approaches are increasingly being employed for the design of Additively Manufactured (AM) parts and are the focus of ongoing research in the AM community. The development of strategies to create complex lattice structures utilising optimal solutions from TO has great potential throughout a wide range of research fields. This investigation explored robustness and effectiveness of proposed design strategies, both in terms of mechanical performance and AM specific design related manufacturing considerations. From the results obtained in this work, the following conclusions can be drawn.

Lattice strategies that are informed by TO results (i.e. Intersected/Graded/Scaled lattices) are considerably (~40–50%) superior in terms of specific stiffness to the structures where this is not the case (i.e. Uniform lattice). The Graded lattice strategy was identified as the most robust strategy from a mechanical performance stand-point due to its high resilience to loading variabilities. For cut members, as is the case with the Intersected and Graded strategies, lattices generated from surface based unit cells were found to be more efficient at transmitting loads when compared to strut based unit cells, essentially because of their higher degree of connectivity.

In principle, a general increasing trend with increased extent of latticing is observed for all the AM specific design related manufacturing considerations investigated, specifically, support structure requirement, processing efforts and design-to-manufacture discrepancy. However, the trend for support requirements can be reversed by employing self-supporting unit cells, giving confidence to the proposed hypothesis i.e. "capturing the geometric complexities that necessitate support gives a good estimate of support requirements for a design".

Although, increased surface area as a result of greater extent of latticing equates to incurring additional processing effort, the relationship is not very straight-forward due to the complexities associated with the surface patch representations and granularity needed to adequately capture regions with lower V_f unit cells. The Graded strategy, as with the findings for the mechanical performance, was identified as being the most robust strategy, as it

Table 6
Quality descriptors indicating most to least promising design strategies for several objectives.

Design Strategy	Optimality – intended loading	Performance Resilient	Support structure requirements	Processing efforts	Design-to-Manufacturing discrepancy
Solid	*Most*	*Somewhat*	*Most*	*Least*	*Least*
Intersected	*More*	*More*	*More*	*Less*	*Somewhat*
Graded	*Somewhat*	*Most*	*Somewhat*	*Somewhat*	*Less*
Scaled	*Less*	*Less*	*Less*	*More*	*More*
Uniform	*Least*	*Least*	*Least*	*Most*	*Most*

was the least affected overall when assessed for design related manufacturing considerations.

The results obtained for the comparative investigation of lattice design strategies, though employing the specific test case of a cantilever beam, are applicable more generally. This is due to the results being largely intrinsic to the design strategy and independent of design parameters chosen. The authors believe that the key findings from this work, summarised qualitatively in Table 6, will help inform engineers and designers about the pros-and-cons of the proposed design strategies, enabling them to make informed choices about the suitability of a strategy for a given design-spec accommodating manufacturing considerations. It is envisaged that this will provide the necessary know-how and in-turn the incentive to realise complex lattice geometries via AM.

Acknowledgment

This work was supported by the Engineering and Physical Sciences Research Council [grant number EP/N010280/1].

References

[1] L.J. Gibson, M.F. Ashby, Cellular Solids: Structure and Properties, Cambridge University Press, 1999.
[2] N.A. Fleck, V.S. Deshpande, M.F. Ashby, Micro-architectured materials: past, present and future, Proc. R. Soc. A Math. Phys. Eng. Sci. 466 (2121) (2010) 2495–2516.
[3] J. Brennan-Craddock, D. Brackett, R. Wildman, R. Hague, The design of impact absorbing structures for additive manufacture, J. Phys.: Conf. Ser. 382 (2012) 12042.
[4] I. Maskery, et al., An investigation into reinforced and functionally graded lattice structures, J. Cell. Plast. 53 (2) (2016) 151–165.
[5] A. Panesar, I. Ashcroft, D. Brackett, R. Wildman, R. Hague, Design framework for multifunctional additive manufacturing: coupled optimization strategy for structures with embedded systems, Addit. Manuf. 16 (2017) 98–106.
[6] G. Ryan, A. Pandit, D.P. Apatsidis, Fabrication methods of porous metals for use in orthopaedic applications, Biomaterials 27 (13) (2006) 2651–2670.
[7] J. Banhart, Manufacture, characterisation and application of cellular metals and metal foams, Prog. Mater. Sci. 46 (6) (2001) 559–632.
[8] Y. Tang, Y.F. Zhao, A survey of the design methods for additive manufacturing to improve functional performance, Rapid Prototyp. J. 22 (3) (2016) 569–590.
[9] D. Wang, Y. Yang, R. Liu, D. Xiao, J. Sun, Study on the designing rules and processability of porous structure based on selective laser melting (SLM), J. Mater. Process. Technol. 213 (10) (2013) 1734–1742.
[10] M.P. Bendsøe, O. Sigmund, Topology Optimization: Theory, Methods, and Applications, 2nd edition, 2003, pp. 724.
[11] A. Panesar, D. Brackett, I. Ashcroft, R. Wildman, R. Hague, Hierarchical remeshing strategies with mesh mapping for topology optimisation, Int. J. Numer. Methods Eng. 111 (7) (2017) 676–700.
[12] J. Kranz, D. Herzog, C. Emmelmann, Design guidelines for laser additive manufacturing of lightweight structures in TiAl6V4, J. Laser Appl. 27 (S1) (2015) S14001.
[13] S.L. Sing, W.Y. Yeong, F.E. Wiria, B.Y. Tay, Characterization of titanium lattice structures fabricated by selective laser melting using an adapted compressive test method, Exp. Mech. 56 (5) (2016) 735–748.
[14] D. Brackett, I. Ashcroft, R. Hague, Topology optimization for additive manufacturing, Solid Free. Fabr. Symp. (2011) 348–362.
[15] L. Cheng, P. Zhang, E. Biyikli, J. Bai, S. Pilz, A. To, Integration of topology optimization with efficient design of addtive manufactured cellular structures, Solid Free. Fabr. Symp. (2015) 1370–1377.
[16] S. Teufelhart, G. Reinhart, Optimization of strut diameters in lattice structures, SFF (2012) 719–733.
[17] D.J. Brackett, I.A. Ashcroft, R.D. Wildman, R.J.M. Hague, An error diffusion based method to generate functionally graded cellular structures, Comput. Struct. 138 (2014) 102–111.
[18] M. Gilbert, A. Tyas, Layout optimization of large-scale pin-jointed frames, Eng. Comput. 20 (8) (2003) 1044–1064.
[19] T. Zegard, G.H. Paulino, GRAND – ground structure based topology optimization for arbitrary 2D domains using MATLAB, Struct. Multidiscip. Optim. 50 (2014) 861–882.
[20] T. Zegard, G.H. Paulino, GRAND3 – ground structure based topology optimization for arbitrary 3D domains using MATLAB, Struct. Multidiscip. Optim. 52 (6) (2015) 1161–1184.
[21] C.J. Smith, M. Gilbert, I. Todd, F. Derguti, Application of layout optimization to the design of additively manufactured metallic components, Struct. Multidiscip. Optim. (2016) 1–17.
[22] J. Nguyen, S.-I. Park, D. Rosen, Heuristic optimization method for cellular structure design of light weight components, Int. J. Precis. Eng. Manuf. 14 (6) (2013) 1071–1078.
[23] M. Alzahrani, S.-K. Choi, D.W. Rosen, Design of truss-like cellular structures using relative density mapping method, Mater. Des. 85 (2015) 349–360.
[24] G.W. Rodgers, E.E.W. Van Houten, R.J. Bianco, R. Besset, T.B.F. Woodfield, Topology optimization of porous lattice structures for orthopaedic implants, IFAC Proc. 19 (2014) 9907–9912.
[25] J.E. Cadman, S. Zhou, Y. Chen, Q. Li, On design of multi-functional microstructural materials, J. Mater. Sci. 48 (1) (2013) 51–66.
[26] Rhinoceros 3D. McNeel, Barcelona, Spain, 2015.
[27] Materialise 3-Matic. Materialise N.V. Leuven, Belgium, 2016.
[28] Simpleware ScanIP. Synopsys, Mountain View, California, U.S., 2016.
[29] Autodesk Within, Autodesk, Inc, San Rafael, CA, USA, 2016.
[30] Altair HyperWorks OptiStruct, Altair Engineering, Inc., Troy, Michigan, U.S, 2016.
[31] "Symvol for Rhino." Uformia, 2014.
[32] A. Hussein, L. Hao, C. Yan, R. Everson, P. Young, Advanced lattice support structures for metal additive manufacturing, J. Mater. Process. Technol. 213 (7) (2013) 1019–1026.
[33] M.P. Bendsoe, Optimal shape design as a material distribution problem, Struct. Optim. 1 (1989) 193–202.
[34] K. Liu, A. Tovar, An efficient 3D topology optimization code written in Matlab, Struct. Multidiscip. Optim. (2014) 1175–1196.
[35] MATLAB R2016a. Mathworks, Massachusetts, USA, Natick, MA, USA, 2016.
[36] A.O. Aremu, et al., A voxel-based method of constructing and skinning conformal and functionally graded lattice structures suitable for additive manufacturing, Addit. Manuf. 13 (2017) 1–13.
[37] S. Rajagopalan, R.A. Robb, Schwarz meets Schwann: design and fabrication of biomorphic and durataxic tissue engineering scaffolds, Med. Image Anal. 10 (5) (2006) 693–712.
[38] MSRI (Mathematical Sciences Research Institute), Triply Periodic Minimal Surfaces, Scientific Graphic Project, 2017 ([Online]. Available: http://www.msri.org/publications/sgp/jim/papers/morphbysymmetry/table/index.html).
[39] MSC Nastran. MSC Software Corporation, California, USA, 2014.
[40] Materialise Magics. Materialise N.V., Leuven, Belgium, 2014.
[41] Autofab Software, Marcam Engineering, 2011.
[42] F. Calignano, Design optimization of supports for overhanging structures in aluminum and titanium alloys by selective laser melting, Mater. Des. 64 (2014) 203–213.
[43] M. Langelaar, Topology optimization of 3D self-supporting structures for additive manufacturing, Addit. Manuf. 12 (2016) 60–70.
[44] G. Reinhart, S. Teufelhart, F. Riss, Investigation of the geometry-dependent anisotropic material behavior of filigree struts in ALM-produced lattice structures, Phys. Procedia 39 (January) (2012) 471–479.